# Effect of Surfactant Chain Length on the Binding Interaction of a Biological Photosensitizer with Cationic Micelles

**Alok Chakrabarty,[†] Paramita Das,[†] Arabinda Mallick,[‡] and Nitin Chattopadhyay*,[†]**

*Department of Chemistry, Jadavpur University, Calcutta 700 032, India, and Division of Frontier Material Science, Graduate School of Engineering Science, Osaka University, Toyonaka 560-8531, Japan*

*Received: October 8, 2007; In Final Form: December 20, 2007*

Steady-state and time-resolved fluorometric techniques have been exploited to study the photophysical and distribution behavior of an efficient cancer cell photosensitizer, norharmane (NHM), in well-characterized, biomimicking nanocavities formed by cationic micelles with varying surfactant chain length. Amphiphiles like dodecyl trimethyl ammonium bromide (DTAB), tetradecyl trimethyl ammonium bromide (TTAB), and cetyl trimethyl ammonium bromide (CTAB) have been used for the purpose. Emission behavior of NHM is very much dependent on the surfactant concentration as well as their hydrophobic chain length. The binding constant ($K$) and free-energy change ($\Delta G$) for the interaction of NHM with the cationic micelles have been determined from the fluorescence data. Polarity of the microenvironment around the probe has been determined in the cationic micellar environments from a comparison of the variation of fluorescence properties of the two-prototropic species of the probe in water/dioxane mixture with varying composition. Experimental results demonstrate that the variation in the cationic surfactant chain length plays an important role in promoting a specific prototropic form of the probe molecule. Fluorescence decays are biexponential in all the micelles indicating that the probe molecules are distributed between the two distinct regions of the micelles. The population of the component with a longer lifetime corresponds to the probe in the head group site, while the short-lived component comes from the probe bound to the core region of the micelles. On the basis of the lifetime measurements, the partitioning behavior of the chromophore in the head group and in the core regions in the micelles has been determined.

## 1. Introduction

There has been a widespread interest in studying the spectroscopic and photophysical properties of fluorescent molecules in different organized media for a better understanding of the solubilization site and interaction in true biological systems. These organized media can mimic reactions in biosystems and also have potential for energy storage.[1] Surfactants, because of their ability to solubilize the membrane proteins, are extremely important in simulating the complex environmental condition present in larger bioaggregates such as biological membranes.[2−4] The wide range of functions performed by the biological membranes and membrane proteins have motivated the researchers to look for simple model systems, which can mimic, at least in part, the physicochemical properties of the membrane architecture. One typical example of such membrane mimetic organized media is micelle which is organized assembly of surfactants in aqueous medium.[5,6] The importance of micelles has been increased rapidly because of their resemblance with proteins, enzymes, and so forth and with mimicking biological systems. Attention has been paid to the micellar activities on the nature and characteristics of different photophysical processes.[2−10] Interest on this aspect has received emphasis in recent years with an explosive growth in research on various bioactive molecules which are promising against a variety of diseases including cancer.[2−10] The photophysical study of the natural product, norharmane (NHM), in different microheterogeneous environments demands a new dimension in chemistry because of its novel biological applications, such as a photosensitizer toward a variety of systems, including bacteria, fungi, viruses, and so forth.[10,11] The use of photosensitizing agents together with light for the treatment of neoplastic diseases, generally known as photodynamic therapy (PDT), has become a topic of increasing medical interest. PDT produces singlet oxygen that is detrimental to the cancerous cells. This is an established modality for cancer treatment.[12] Norharmane has been reported to be quite effective in producing singlet oxygen, and it could be used as an efficient cancer cell photosensitizer.[13] The extent of photodynamic action depends not only on the singlet oxygen production but also on the biodistribution of the probe molecule in the cytoplasmic and mitochondrial membranes and on the retention and the nature of the binding inside the cell. Thus, it is important to specify the location of the probe molecules in a microheterogeneous environment. Study of the binding interaction of NHM with different biosystems/organized media thus becomes important for studying the net PDT efficiency. The photophysical and photochemical properties of NHM have been shown to be strongly modified by the solvents.[14−16] In aqueous solution, NHM exists in four different forms (neutral, cation, anion, and zwitterion) depending on the pH of the medium. The spectroscopic details of the individual species have been reported by several groups.[14−16] The various acid−base equilibria for NHM have been presented in Scheme 1.

Much photophysical, biochemical, and biological research has been performed using norharmane as a probe.[17−25] Some recent literature projects that in aqueous medium, protonation of this

* To whom correspondence should be addressed. Fax: 91-33-24146266. E-mail: pcnitin@yahoo.com.
[†] Jadavpur University.
[‡] Osaka University.

10.1021/jp709818d CCC: $40.75 
Published on Web 02/29/2008

**SCHEME 1: Different Acid−Base Equilibria for Norharmane**[a]

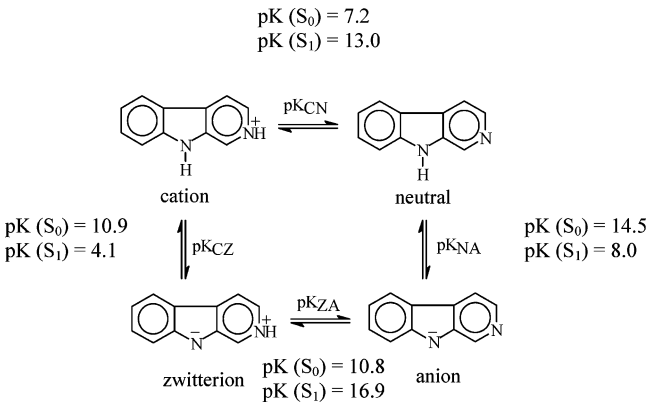


[a] CN, cation−neutral; NA, neutral−anion; ZA, zwitterion−anion; CZ, cation−zwitterion. p*K* values are taken from ref 16.

molecule is important in excited singlet[24] and triplet states.[21] Both triplet state formation and singlet oxygen photosensitization decrease on protonation of the molecule.[21] The structure and the function of such biologically active molecules draw attention of the researchers because of their ability to achieve specific chemical efficiency as a result of organization in the reaction media. For a particular prototropic probe, it is often necessary to opt for one prototopic form or for a desired composition of the different prototropic species for achieving better efficiency for a targeted purpose in a specific environment. Recently, triplet state studies on some $\beta$-carboline molecules by Varela et al.[21] reveal that in their neutral forms these compounds have significant triplet state yield and that the long-lived triplet states may play an important role in their photosensitization reactions in vivo in the presence of oxygen. In contrast to the situation with the availability of many photophysical data, relatively little has been published on the modulation of the prototropic equilibrium and biodistribution of this group of molecules in different biomimetic environments. This is definitely a surprising omission. Considering the possible role of the prototropic forms and the importance of the biodistribution of these molecules in their photosensitization reactions, we have been interested in addressing these aspects. Recent reports demonstrate the effect of the alkyl chain length on the photophysics of different fluorophores as well as on the solvation dynamics in cationic and anionic micellar environments.[26,27] In one of our previous attempts, we monitored the modulation of the prototropic equilibrium of norharmane in anionic micellar environments in the ground state through a variation in the surfactant chain length.[17] The present study in cationic micelles intends to touch some of the unaddressed aspects with a special emphasis on the biodistribution of the sensitizer molecule in different microscopic regions in the micellar microheterogeneous environments. The basic intention of the present study is to explore the potential usefulness of the spectroscopic properties of this photosensitizer molecule, understanding the switching between the different prototropic forms of this molecule, and also to know the biodistribution of this photosensitizer in membrane mimetic cationic micellar environments formed from surfactants with varying chain length.

## 2. Experimental Section

Norharmane procured from Aldrich Chemicals was purified by recrystallization from ethanol. Dodecyl trimethyl ammonium bromide (DTAB), tetradecyl trimethyl ammonium bromide (TTAB), and cetyl trimethyl ammonium bromide (CTAB) were used as received from Aldrich. Analytical grade urea (SRL, India) was used without further purification for the denaturation study. Spectroscopic grade 1,4-dioxane (Aldrich) was used for the polarity measurement experiments. Triply distilled water was used throughout the experiment. For the entire experiment, the concentration of NHM was $2 \times 10^{-5}$ M. pH of the aqueous experimental solutions was measured using a Systronics digital $\mu$-pH meter (model 361).

Shimadzu UV-1700 absorption spectrophotometer and Spex fluorolog-2 spectrofluorimeter were used for the absorption and emission spectral studies, respectively, at 300 K. For the steady-state fluorometric measurements, the fluorophore was excited at 350 nm so as to excite principally the neutral species of NHM in the ground state.[17] Fluorescence lifetimes were determined from time-resolved intensity decay by the method of time-correlated single photon counting (TCSPC) using a nanosecond diode (IBH, U.K. nanoLED-03) as the light source at 370 nm. The typical response of this excitation source is 1.2 ns. The decay curves were analyzed using IBH DAS-6 decay analysis software. The quality of fits was judged from $\chi^2$ criterion and visual inspection of the residuals of the fitted function to the data. The lifetimes were measured in air-equilibrated solution at ambient temperature (300 K). Mean (average) fluorescence lifetimes ($\langle\tau\rangle$) for biexponential iterative fittings were calculated from the decay times and the pre-exponential factors using the following relation:

$$\langle\tau\rangle = a_1\tau_1 + a_2\tau_2 \quad (1)$$

where $a_1$ and $a_2$ are the normalized pre-exponential factors and $\tau_1$ and $\tau_2$ are the corresponding lifetime values.

## 3. Results and Discussion

**3.1. Absorption Study.** The absorption spectrum of NHM in aqueous medium shows two bands with maxima at 372 and 348 nm corresponding to the cationic and the neutral species, respectively.[16,18] With the addition of DTAB, TTAB, and CTAB separately to the air-equilibrated aqueous solution of NHM, the absorption spectra of the fluorophore show only minor changes. Figure 1 depicts the variation of the absorption spectra of NHM in the three cationic micelles. Up to critical micellar concentration (CMC) of the surfactants, the cationic band shows a slight increment with a small decrease in the neutral band. On the other hand, after attainment of CMC, small decrease in the cationic band is observed with concomitant increase in the neutral band of NHM.

Explanation for the spectral changes below CMC is not available at the moment. Premicellar interaction might be responsible for the same. However, after the CMC, the prototropic equilibrium of NHM favors the neutral species of the fluorophore, disfavoring the cationic species, which is expected considering the cationic surface charge of the micelles studied.

**3.2. Emission Study.** Room-temperature emission spectrum of NHM in aqueous solution shows a single and unstructured band peaking at 450 nm ascribed to the cationic species.[16−18] Gradual addition of the surfactant (DTAB, TTAB, or CTAB) to the solution changes the emission spectrum drastically. A new blue-shifted emission band with peak at 380 nm develops at the cost of the 450 nm emission resulting in an isoemissive point at ~409 nm in all the three micellar solutions. Figure 2 depicts the emission spectra of NHM as a function of the concentration of the three surfactants. Consistent with the

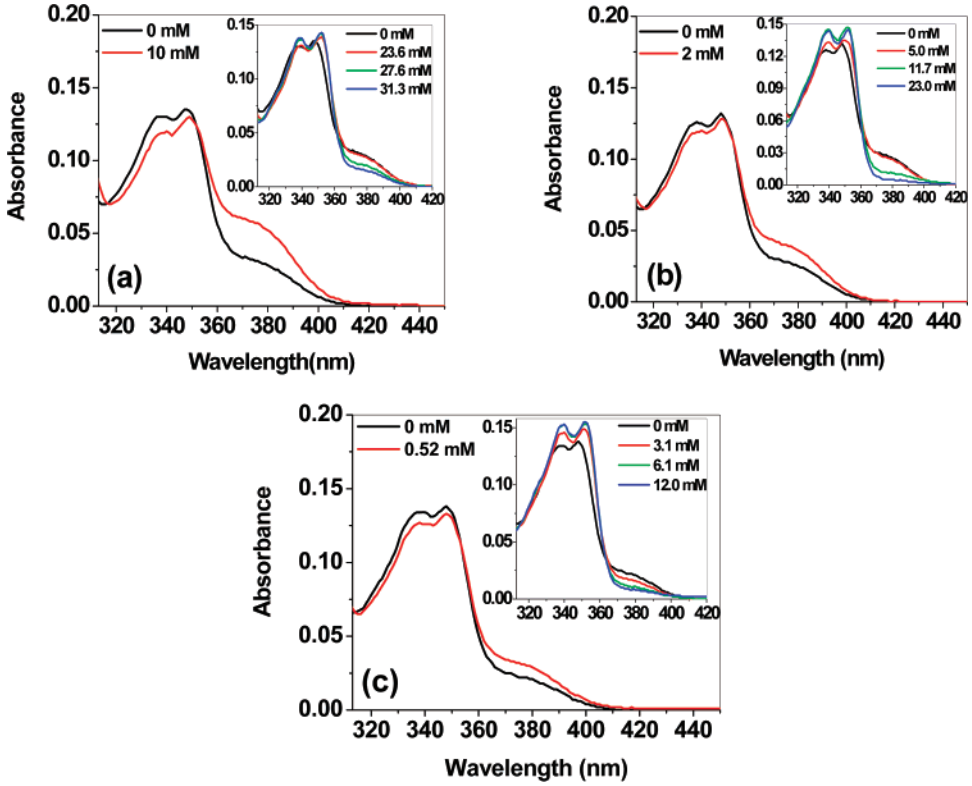


**Figure 1.** Absorption spectra of NHM in (a) DTAB, (b) TTAB, and (c) CTAB solutions below their respective critical micellar concentrations (CMC). Insets show the absorption spectra of NHM above the CMC values of the individual surfactants.

existing literature, the 380 nm fluorescence band has been assigned to the neutral species of NHM.[16,17]

Observation of the isoemissive point substantiates that the prototropic interconversion is limited within the cationic and the neutral species only in all the micelles studied. Plots of the ratio of neutral to cation band intensity against the surfactant concentration reveal break points around the respective critical micellar concentrations (CMC) (Table 1). Figure 2 reflects that the basic pattern of modification in the observation with the addition of the surfactants is alike for all the cases studied here with some difference from a quantitative point of view. The relative enhancements of the neutral to the cationic emission at the respective saturation levels appear to be in the order DTAB > TTAB > CTAB (see insets of Figure 2). The equilibrium between the cationic and the neutral species of NHM can be readily understood by the measurement of the equilibrium constants and the free-energy changes at various concentrations of the surfactants used. Since the micellar phase is silent from a spectroscopic point of view, the effect of surfactant molecules on the prototropic equilibrium is reflected through the changes in the spectral properties of the probe molecule itself. Ratios of the fluorescence intensities and fluorescence quantum yield of neutral and cationic species provide the ratio of concentrations of the respective species enabling one to estimate the equilibrium constant ($K_{eq}$), considering a constancy of the molar extinction coefficient as the fluorophore is excited at 350 nm, where both the neutral and cationic species coexist in equilibrium. The prototropic equilibrium can be represented as

$$\text{cation (C)} \rightleftarrows \text{neutral (N)} \tag{2}$$

and the equilibrium constant ($K_{eq}$) can be represented as

$$K_{eq} = \frac{[N]}{[C]} \tag{3}$$

where [N] and [C] represent the concentrations of the neutral and the cationic species, respectively. The free-energy change corresponding to the above equilibrium can then be determined from the following relation:

$$\Delta G = -RT \ln K_{eq} \tag{4}$$

Figure 3 shows the variation of the equilibrium constant ($K_{eq}$) and the corresponding free-energy change ($\Delta G$) with increasing surfactant concentration for the three-surfactant systems studied.

From Figure 3, it is evident that as the surfactant concentration increases the prototropic equilibrium moves toward the neutral species for all the surfactant systems studied. It is further noted that the $\Delta G$ value at the saturation levels of the probe−micelle interaction becomes less negative as the surfactant chain length increases, which concludes that the switchover from the cationic to the neutral form is disfavored with increasing hydrophobic chain length. In one of our recent reports on the same molecular system, we showed that polar and protic solvents (capable of donating proton) have specific influence on the photophysics of NHM.[25] Thus, in water, NHM gives only cationic emission while in pure dioxane only the neutral emission exists. A fluorometric study in a varying composition of water/dioxane mixture shows a similar enhancement of the neutral emission of NHM and a concomitant decrease in the corresponding cationic emission when the dioxane proportion is increased in the solvent mixture. The study indicates that the neutral species of NHM prefers to reside in a more hydrophobic region where proton transfer is rather restricted. A similar observation is noticed here also for the addition of the individual surfactants. On the basis of the above discussion, one can presume that an increase in the chain length of the surfactant, promoting the hydrophobicity factor, should favor the excited-state prototropic equilibrium toward the neutral species. Practically, we observed the reverse; the increase in chain length disfavors this prototropic transformation.

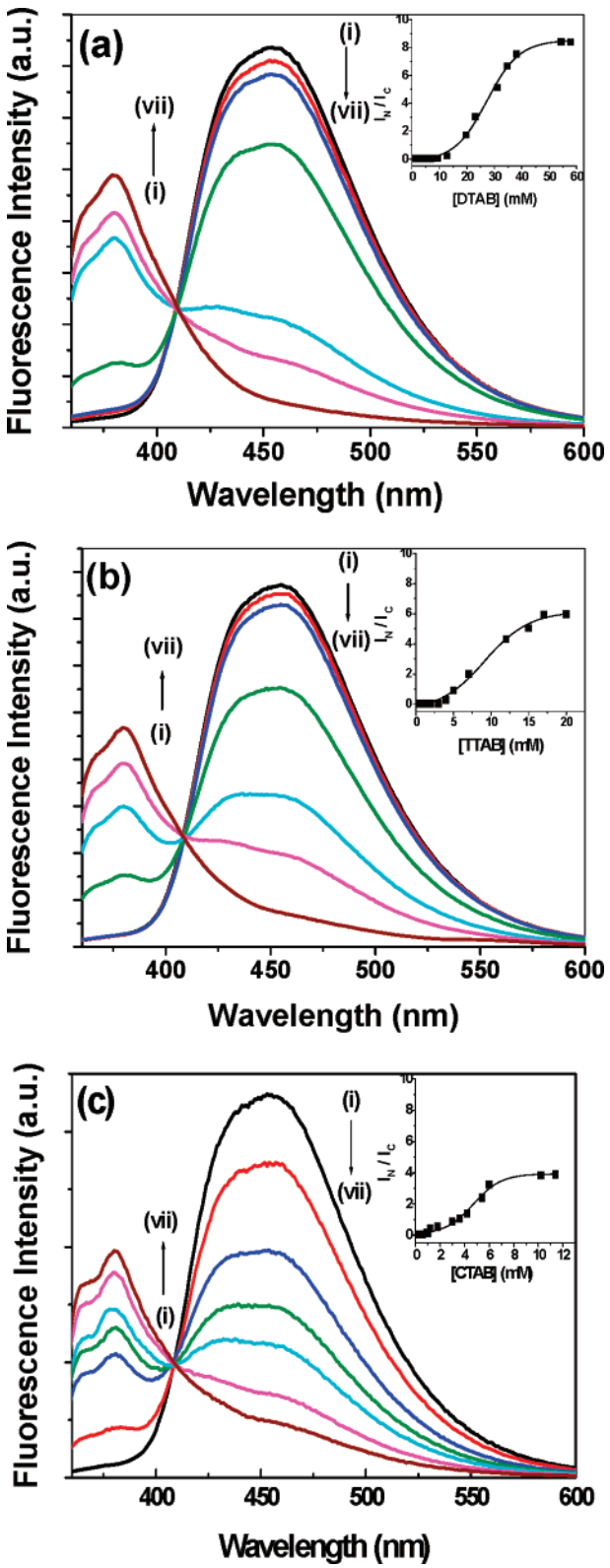


**Figure 2.** Emission spectra of NHM solutions as a function of (a) DTAB, (b) TTAB, and (c) CTAB concentrations ($\lambda_{exc}$= 350). Curves i→vii correspond to 0.0, 9.2, 12.7, 15.0, 19.6, 23.1, and 54.3 mM in a; 0.0, 2.0, 3.0, 4.0, 5.0, 10.0, and 20.0 mM in b; and 0.0, 0.9, 1.8, 3.0, 4.8, 7.2, and 11.4 mM in c. Insets show the variations of the fluorescence intensity ratio of neutral to cation band of NHM in the respective media as a function of surfactant concentration.

Apparent anomalous behavior was also reported by our group while investigating the photophysics of NHM in anionic micellar systems having different chain length.[17] Fluorometric study reflected that in all the three micellar environments studied

**TABLE 1: Literature Values of CMC and Aggregation Number of the Investigated Surfactant Systems**

| surfactants | CMC (mM)[a] | aggregation number[a] |
|---|---|---|
| DTAB | 15 | 50 |
| TTAB | 3.5 | 67 |
| CTAB | 0.8 | 92 |

[a] From ref 28.

therein only the protonated form was present. It was also established that the prototropic equilibrium from neutral to cation in the ground state is sensitive to the chain length of the surfactant and is quite different from the normal expectation. The results were rationalized in terms of the local pH and the surface charge of the micellar units. In the anionic micellar systems, the negative surface charge is supposed to play an important role to favor the protonated species. This is not the case in cationic and nonionic micelles.[18,30] In the latter cases and in serum albumin environments,[25] the observations can grossly be rationalized considering the degree of probe penetration. The effect of variation of surfactant chain length in the present case of cationic micellar environments might be interpreted from a similar consideration together with the compactness factor of the micellar units.

It is known that water can enter within the micelles up to a certain depth[30−32] depending on the compactness of the micellar units. Thus, micelles with compact head groups suffer a smaller water penetration compared to the micelles with less compact head groups. In this regard, it is important to note that neutron scattering experiments on micelles having different surfactant chain lengths reveal that the head group structures of the micelles differ significantly.[31,32] As an example, in DTAB water penetrates into the head group region to a depth of ∼4 carbons, whereas in TTAB water penetrates in ∼2.5 carbons.[30] This observation reveals that the compactness of the head group increases with an increase in the surfactant chain length. Arguing in the same line, as we move from DTAB to CTAB, the increased chain length enhances the compactness of the head group gradually, which in turn decreases the extent of water penetration (micellar hydration).[27] This is expected to favor the equilibrium toward the neutral form of NHM (because of low polarity) rather than the cationic species contrary to the experimental findings. The model of water penetration/micellar hydration, failing to explain the experimental observations, is thus ruled out to act as the dominating factor here.

Another plausible factor possibly responsible for a switching between the two prototropic forms of NHM is ascribed to the local pH at the micellar surface. It is, however, known that within the pH range 1−11 only cation and neutral forms exist in the ground state while in the same pH range only cationic species exists in the excited state.[14,15] In the present situation, addition of the different surfactants is not supposed to change the pH so drastically to move it beyond this range (measurement of the bulk pH reflects only a nominal change). Thus, a change in the local pH at the micellar surface (with the variation in surfactant chain length) is not believed to be responsible for the transformation of cation to the neutral species of NHM. Screening from all plausible considerations, we are thus left with the postulate of the degree of probe penetration into the micellar nanocavity and the micellar compactness to rationalize the experimental findings.[33] The increase in surfactant chain length increases micellar compactness; micelles with compact head groups suffer a smaller probe penetration compared to the micelles with less compact head groups[34] which prevents the incorporation of the probe molecules into a deeper inside, which

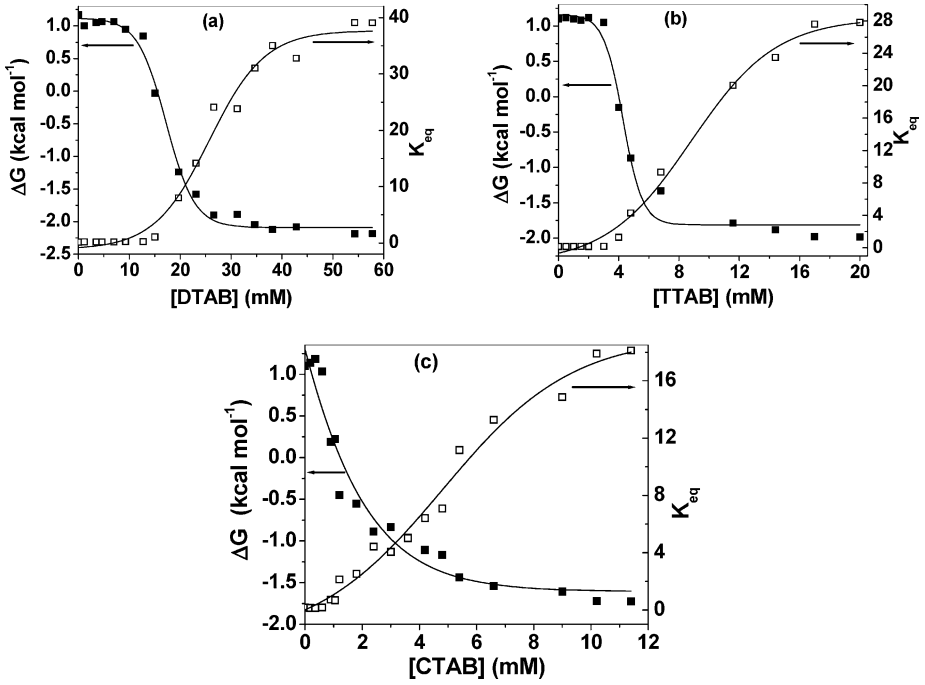


**Figure 3.** Variation of equilibrium constant and free-energy change as a function of (a) DTAB, (b) TTAB, and (c) CTAB concentrations.

in turn enhances the population of the cationic species with an increase in the surfactant chain length.

**3.3. Probe−Micelle Binding.** The usefulness of biologically active molecules as therapeutic agents is basically dependent on their binding abilities. This also influences the drug stability and toxicity during their chemotherapeutic process. Keeping this in mind, the binding constants between the probe and the cationic micelles have been determined from the fluorescence intensity data for the individual species of NHM following the method described by Almgren et al.[34] We have

$$[(I_\infty - I_0)/(I_c - I_0)] - 1 = (K[M])^{-1} \quad (5)$$

where $I_0$, $I_c$, and $I_\infty$ are the fluorescence intensities of the particular species of NHM considered in the absence of surfactant at an intermediate surfactant concentration and at a condition of complete interaction, respectively, $K$ being the binding constant and [M] the micellar concentration. The micellar concentration [M] is determined by

$$[M] = ([S] - CMC)/N \quad (6)$$

where [S] represents the surfactant concentration and $N$ is the aggregation number of a micellar system. From the work of Weidemaier et al.,[28] the values of $N$ for DTAB, TTAB, and CTAB have been taken as 50, 67, and 92 (see Table 1). The binding constant ($K$) values have been determined from the slopes of the plots of $[(I_\infty - I_0)/(I_c - I_0)] - 1$ against $[M]^{-1}$ (Figure 4). From the $K$ values, the free-energy changes for the probe−micelle binding process have been calculated for the three micellar systems at ambient temperature. The values are presented in Table 2.

The binding constants and free-energy data were calculated considering both cationic and neutral species of NHM individually. The values considering the neutral and the cationic species corroborate each other. Figure 4 and Table 2 present the data corresponding to the neutral species. The estimated binding constant values (±15%) are in the range of values for some other systems reported earlier.[35]

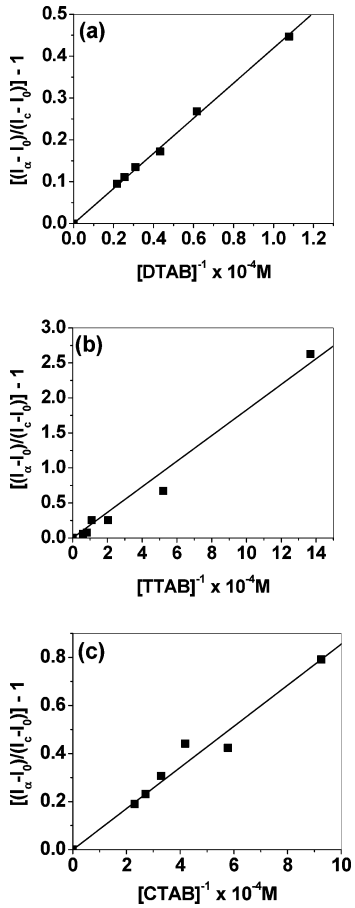


**Figure 4.** Plot of $(I_\infty - I_0)/(I_c - I_0) - 1$ against $[M]^{-1}$ in (a) DTAB, (b) TTAB, and (c) CTAB (for details see text).

**3.4. Polarity of the Micellar Microenvironments.** For a couple of decades, fluorescent probes have been serving a unique role in the determination of the microscopic polarity of the biological and biomimicking environments.[18,20,25,31,36,37] The polarity determined through different photophysical parameters of the probe gives a relative measure of the polarity of the

**TABLE 2: Binding Constants and Free-Energy Changes for NHM−Micelles Interaction**

| surfactants | binding constant ($K$) $\times 10^{-4}$ (lit mol$^{-1}$) | $\Delta G$ (kJ mol$^{-1}$) |
|---|---|---|
| DTAB | 2.38 | −25.14 |
| TTAB | 5.47 | −27.21 |
| CTAB | 11.69 | −29.11 |

microenvironment next to the probe. Local polarity around a probe in biomimetic environments can be estimated by comparison of the spectral properties of the fluorophore in that environment with those of the probe in pure solvents or in solvent mixtures of known polarities.[18,20,37] It is true that the polarity of a homogeneous environment is not exactly the same as the polarity in a microheterogeneous medium. However, to have a qualitative estimate, polarities in the microheterogeneous environments like micelles, reverse micelles, proteins, and lipids are often determined and expressed in polarity equivalent $E_T$-(30) scale comparing the fluorescence behavior of the probe in microheterogeneous environments to that in a mixture of homogeneous solvents of varying composition.[18,20,37−39] To get a measure of the polarity at the binding site of the micelle with the fluorophore empirical solvent polarity parameter, $E_T(30)$, the transition energy for the solvatochromic intramolecular charge transfer absorption of the betaine dye 2,6-diphenyl-4-(2,4,6 triphenyl-1-pyridino) phenolate as developed by Reichardt was used.[39,40] Since the probe has dual fluorescence in micellar environments, it is logical to consider the fluorometric properties of both the neutral and the cationic species to get an approximate polarity around the probe molecule. Thus, a calibration curve was constructed monitoring the log of the neutral to cation fluorescence intensity of NHM in water/dioxane mixture versus $E_T(30)$ (Figure 5). Here, a linear relationship was obtained between the two parameters. Similar correlations are also known for other simple organic solvents like methanol. However, neutral/cation fluorescence intensity ratios in the studied micellar solutions are more than that in methanol. This indicates that the polarity within the micelles is less than that in methanol. Since dioxane−water mixture covers a much wider range of polarity, we have exploited this mixture for our purpose.

By interpolating the values of the log of the neutral to cation intensity ratio of NHM at a situation when the probe−micelle interaction is complete (DTAB: 60 mM, TTAB: 20 mM, and CTAB: 12 mM) on the calibration plot, the micropolarities around the probe were found to be 53.2, 53.8, and 54.4 for the said systems, respectively. From the micropolarity values, it is clear that the probe is located in more hydrophobic region in DTAB than in TTAB and CTAB. The polarity values corroborate our steady-state fluorescence study where the relative increment of the neutral band intensity was in the order DTAB > TTAB > CTAB.

**3.5. Action of Urea.** The interest of the study of the effect of urea on photophysical and photochemical processes of probes in different microheterogeneous environments stems from the denaturing action of urea toward proteins. Since micelles are relatively simple models for complex biological systems and the transition of protein from a disordered state to the native conformation has some resemblance to micelle formation, many recent studies have been undertaken to elucidate the action of urea on the micellization and demicellization processes. To explain the role of urea as denaturant, two propositions have been put forward. According to the first proposition, urea breaks the liquid structure of water, and the other proposition dictates that urea displaces some water molecules from the periphery of the microheterogeneous units like micelles, protein, and so forth which eventually modifies the solvation of the solute fluorophore. Surface tension measurement[41] and computer simulation[42] support the second proposition. In general, chaotropes such as urea perturb the organization of molecular assemblies whose formation is driven by the hydrophobic effect.[43,44] This is due to their ability to weaken hydrophobic forces in aqueous solution. It is therefore expected that chemical agents such as urea will influence the organization and stability of the assemblies that are determined by the delicate balance between hydrophilic and hydrophobic forces. To get some insight regarding the action of urea and how surfactant chain length influences this action, we have studied the action of urea to the NHM bound micelles varying the chain length of the surfactants, that is, changing the hydrophobicity. The fluorescence spectrum of micelle-bound NHM (Figure 2) shows a decreased cationic emission at 450 nm for all the cases (DTAB, TTAB, and CTAB) and an enhanced neutral emission at 380 nm. On gradual addition of urea to the micelle-bound NHM, the emission profile undergoes a significant change opposite to the observation reflected in Figure 2 (data not shown), that is, decrease in neutral band intensity with a concomitant increase in the cationic band intensity. The reverse pattern in the variation of the fluorescence spectrum with respect to Figure 2 upon addition of urea remains unexplained unless and until we assume that urea causes a decrease in the number of fluorophores bound to the micelles.[45] For a clear understanding of the effect of surfactant chain length on this phenomenon, we have presented a bar diagram (Figure 6) of the ratio of cationic fluorescence intensity to that of the neutral fluorescence intensity in the presence of a definite amount of urea (8 M). Figure 6 depicts the difference in the effectivity of urea toward denaturation of the three micellar systems.

From the above observation, it is apparent that urea eradicates NHM more efficiently from DTAB environment than from TTAB and CTAB. This can be explained on the basis of the water penetration model in the micellar systems as follows. As revealed by Berr et al.,[32] the compactness of the micellar units with an increase in the surfactant chain length follows the order

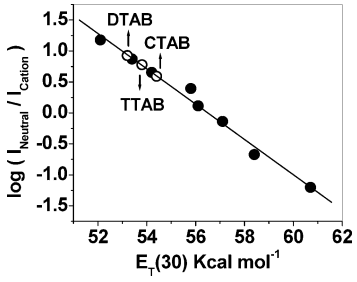


**Figure 5.** Variation of log of neutral to cation fluorescence intensity ratio of NHM in water/dioxane mixture against $E_T(30)$. The experimental values of the former parameter in DTAB, TTAB, and CTAB environments have been incorporated in the figure.

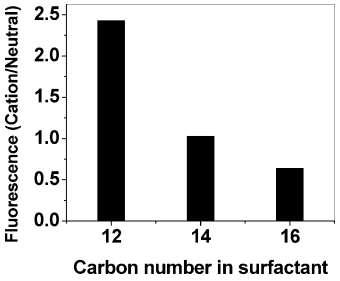


**Figure 6.** Recovered fluorescence intensity ratio (cation/neutral) as a function of surfactant chain length in the presence of 8 M urea. [DTAB] = 60 mM, [TTAB] = 20 mM, and [CTAB] = 12 mM.

**TABLE 3: Lifetime of NHM in Aqueous and Different Micellar Environments**

| environment | $a_1$ | $\tau_1$ (ns) | $a_2$ | $\tau_2$ (ns) | $\langle\tau_f\rangle$ (ns) | $\chi^2$ |
|---|---|---|---|---|---|---|
| water | | 20.0 | | | 20.0 | 1.16 |
| DTAB (60 mM) | 0.286 | 16.75 | 0.714 | 1.36 | 5.76 | 1.27 |
| TTAB (20 mM) | 0.679 | 20.36 | 0.321 | 1.23 | 14.22 | 1.14 |
| CTAB (12 mM) | 0.896 | 21.01 | 0.104 | 1.40 | 18.97 | 1.17 |

DTAB < TTAB < CTAB. The greater the compactness is, the lesser will be the water penetration. So, DTAB suffers a higher degree of water penetration than TTAB and CTAB. Urea eradicates the water molecules adjacent to the micellar environments and will destabilize the microenvironments. This, in turn, facilitates the desolvation of the guest fluorophore molecules leading to the release of them from the micellar region to the bulk aqueous phase and results in a relative increase in the cationic fluorescence. This observation also substantiates the binding phenomenon discussed in section 3.3.

**3.6. Time-Resolved Fluorescence Study: Implication on the Distribution of the Probe.** Fluorescence lifetimes of NHM have been measured at the saturation level of NHM−micelle interaction (this corresponds to high concentration of the surfactants) and are presented in Table 3. The specific concentrations used for the micelles are indicated therein. These concentrations were chosen as the addition of further amount of surfactants failed to bring any noticeable change in the spectral pattern or lifetime. Excited-state lifetime measurements provide sensitive parameters for exploring the local environment around a fluorophore and also provide information on the probe−micelle interactions.[46−49] For the same reason that the emission spectra of the fluorophores are sensitive to the local environment, their fluorescence lifetimes reflect intermolecular interactions. A single-exponential fluorescence decay indicates that the fluorescent species exists in a single environment or that there is a rapid exchange between the multiple environments over the time scale of measurement.[48−51] A deviation from the single-exponential decay behavior indicates that the fluorescent probe exists in multistable environments where exchange is slow or where simultaneous relaxation from the multiple excited electronic states occurs.[49−52] It is imperative from the above account that the time-resolved fluorescence technique could provide valuable information regarding the location and distribution of a probe molecule in complex microheterogeneous environments in a better way. In water, NHM exhibits a single-exponential decay with a lifetime of around 20 ns, but in all the micellar environments studied, the decay becomes biexponential. Such a behavior may be attributed to the differential distribution of the probe molecules in the micellar environments.[48−51] Typical biexponential decay profiles of NHM in micellar environments are shown in Figure 7. The fluorescence lifetimes of NHM in water and different micellar environments are tabulated in Table 3.

From Table 3, it is clear that the decay parameters are affected by the increased chain length of the surfactants constituting the micellar microenvironments. The fluorescence decay is characterized by a longer decay component with lifetime ($\tau_1$) in the range of 16−21 ns and a relatively shorter component ($\tau_2$) in the range of 1.2−1.4 ns. In the micellar environments, the longer-lived component has a lifetime close to the lifetime of the probe in aqueous medium whereas the shorter component is significantly different. Observation of two widely different time constants in the fluorescence decays implies the existence of two dynamical processes that occur on different time scales and suggests the distribution of the probe in two different microenvironments. The obvious possibility is that the slow and

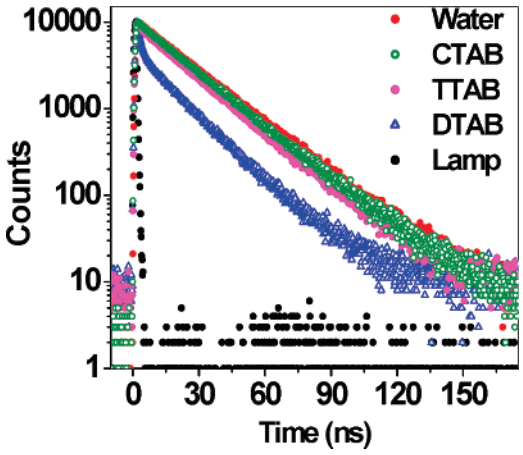


**Figure 7.** Time-resolved fluorescence intensity decays of NHM in water and in different micelles. ($\lambda_{exc}$ = 370 nm, $\lambda_{em}$ = 450 nm). Inset shows the respective environments.

the fast components in the fluorescence decay arise from the distribution of the dye in the bulk water and in the micelles, respectively. The closeness of the long component in case of TTAB and CTAB with that in water also strengthens this proposition. Had this proposition been correct, the ratio $a_1/a_2$ would then give the ratio of the free and the bound dye. To check the acceptability of this concept, we have calculated the relative amount of free and micelle-bound probe from the following relation using the determined binding constant values at the saturation level of NHM−micelle interaction (specific surfactant concentrations are mentioned in Table 3).

$$[\mathrm{NHM}]_0 = [\mathrm{NHM}]_T/(1 + K[\mathrm{M}]) \quad (7)$$

where $[\mathrm{NHM}]_0$ and $[\mathrm{NHM}]_T$ are concentrations of free and total NHM, respectively. [M] is the micellar concentration, and $K$ is the binding constant, respectively. Calculation suggests that more than 93% of probe molecules are bound with the micelles in all these cases. From a glance at Table 3, one can easily feel that the calculated ratios (free to micelle-bound probe) are remarkably less than the $a_1/a_2$ ratios obtained from the fluorescence decay analyses. On the basis of the above observation, we believe that in the present case the fluorescence decay in micelles is only due to the dynamics of the dye bound to micelles and does not correspond to the free dye. Consideration of the relative concentrations of the probe to the surfactants approves this proposition. A significant difference in the measured polarity parameter in terms of $E_T(30)$ around the probe in the micelles (53−54) from that of bulk water (63.1) also supports this conjecture. In tune with the many recent reports, we explain the biexponential character of the fluorescence decays in the micellar environments in terms of partitioning of the probe between two distinct environments within the micelles.[49−52]As is known, micelles are characterized by three distinct regions: a nonpolar core formed by the hydrocarbon tails of the surfactant, a compact stern layer having the head groups, and a relatively wider Gouy−Chapman layer containing the counterions.[52] Depending on the nature of the probe and the micelle, a probe molecule can bind either to the head group region or to the nonpolar core of the micelles. The two microenvironments (the Stern layer and the core region) of a micelle have quite different properties. The core region is usually characterized by highly viscous hydrocarbon-like environment with a very low degree of water penetration. The Stern layer mainly consists of polar head groups, bound counterions, and largely structured water molecules. Because of the differences

in the properties of the head group region and the core region of micelles, different types of molecules are expected to be located selectively in the two regions. If the chromophore resides in a single site, then a single-exponential decay is generally expected. It is pertinent to mention here that in our previous study with the same molecular system in different anionic micelles we observed single-exponential decays and we attributed the observation in terms of the single-site solubilization.[17] Biexponential fluorescence decays in the present experiment envisage that the probe molecule is partitioned between the head group region and the core region of the micelles contrary to its solubilization in a single site. Often, the interfacial and the core regions of aqueous micelles resemble water/alkanol and dioxane-like environments, respectively.[33,50,52] We have determined the lifetime of NHM in methanol and dioxane media. The decay curves are best fitted by single exponential in both the cases, and the lifetimes are determined to be 20 and 2.3 ns, respectively, quite similar to the decay times analyzed in the micellar solutions. Keeping parity with all these points, the longer decay component of the probe molecule in micellar environments is assigned to the species present in the Stern layer of the micelles while the shorter decay component is assigned to the species present in the core. Matzinger et al.[50] have addressed this issue using 2-(*N*-hexadecylamino)-naphthalene-6-sulfonate (HANS) and 2-(*N*-decylamino)-naphthalene-6-sulfonate (DANS) as chromophores in DTAB, TTAB, and CTAB and in the corresponding chloride micellar environments. On the basis of their detailed study, they ascribed their observation of biexponential decays in micelles to the dual solubilization of the probe molecules in the head group region and the core region. Later, Cang et al.[51] and Shannigrahi and Bagchi[33] also presented a similar explanation while rationalizing the fluorescence decay behavior of various probes in different micelles of similar nature. It is encouraging to note that the contribution of the short-lived component in the present experiment decreases substantially as we move toward surfactants of longer chain length. This is ascribed to the enhanced compactness of the micellar units as we move from DTAB to CTAB through TTAB. Thus, as we move to higher hydrophobic chain length, the enhanced compactness of the micellar units prevents the entrance of the probe into the core region which in turn increases the contribution of the longer-lived component significantly. Further, a simple calculation reveals that at the saturation concentrations of the micelles (60 mM for DTAB, 20 mM for TTAB, and 12 mM for CTAB) the number density of the micellar units decreases from DTAB to CTAB because of the gradual increase in the aggregation number. This also goes in favor of supporting the observation of a gradual decrease in the amount of shorter-lived species from DTAB to CTAB. Partitioning of the probe between the head group and the core regions of the micelle can be estimated from the relative contribution of the species toward the fluorescence decay following the model proposed by Matzinger et al.[50] According to the model, the partition coefficient ($P$) between the head group and the core region is given by

$$P = [\mathrm{NHM}]_{\mathrm{Stern}}/[\mathrm{NHM}]_{\mathrm{core}} = a_1/a_2 \qquad (8)$$

Following eq 8, the partition coefficient values have been determined, and they are 0.4, 2.1, and 8.6 for DTAB, TTAB, and CTAB, respectively.

## Conclusion

The present work reports the effect of increased chain length of surfactants capable of forming cationic micelles on the photophysics of a polarity sensitive biological photosensitizer, norharmane. Steady-state and time-resolved fluorometric studies reveal that the prototropic equilibrium shifts toward the cationic species with an increase in the hydrophobic chain length. The time-resolved fluorescence decay analyses suggest that the probe is partitioned between the interfacial and the core regions. An increase in the surfactant chain length increases the compactness of the micellar units leading to an increase in the population of the probe residing in the interfacial region relative to that in the core region of the micellar environments. The work also demonstrates the differential effect of urea on the micellar systems having the same head group but differing in the alkyl chain length.

**Acknowledgment.** Financial supports from DST and DBT, Government of India, are gratefully acknowledged. P.D. is thankful to CSIR for the fellowship.

## References and Notes

(1) Fendler, J. H. *Membrane Mimetic Chemistry*; Wiley-Interscience: New York, 1982.
(2) *Photochemistry in Organised and Constrained Media*; Rammurthy, V., Ed.; VCH: New York, 1991.
(3) *Surfactants in Solution*; Mittal, K. L., Lindman, B., Eds.; Plenum: New York, 1984; Vols. 1−3.
(4) Moulik, S. P. *Curr. Sci.* **1996**, *71*, 368.
(5) Haldar, B.; Chakrbarty, A.; Mallick, A.; Mandal, M. C.; Das, P.; Chattopadhyay, N. *Langmuir* **2006**, *22*, 3514.
(6) Becker, R. S.; Ferreira, L. F. V.; Elisei, F.; Machado, I.; Latterini, L. *Photochem. Photobiol.* **2005**, *81*, 1195.
(7) Schillén, K.; Anghel, D.; Miguel, M. G.; Lindman, B. *Langmuir* **2000**, *16*, 10528.
(8) Bhattacharya, K.; Chowdhury, M. *Chem. Rev.* **1993**, *93*, 507.
(9) Shannigrahi, M.; Bagchi, S. *J. Phys. Chem. B* **2004**, *108*, 17703.
(10) Deepa, S.; Mishra, A. K. *J. Pharm. Biomed. Anal.* **2005**, *38*, 556.
(11) Dias, A.; Varela, A. P.; Miguel, M. G.; Maçanita, A. L.; Becker, R. S. *J. Phys. Chem.* **1992**, *96*, 10290.
(12) Varela, A. P.; Miguel, M. G.; Maçanita, A. L.; Becker, R. S.; Burrows, H. D. *J. Phys. Chem.* **1995**, *99*, 16093.
(13) Chae, K. H.; Ham, H. S. *Bull. Korean Chem. Soc.* **1987**, *7*, 478.
(14) Sakurovs, R.; Ghiggino, K. P. *J. Photochem.* **1982**, *18*, 1.
(15) Reyman, D.; Vinas, M. H.; Poyato, J. M. L.; Pardo, A. *J. Phys. Chem. A* **1997**, *101*, 768.
(16) Vert, F. T.; Sanchez, I. Z.; Torrent, A. O. *J. Photochem.* **1983**, *23*, 355.
(17) Chakrabarty, A.; Mallick, A.; Haldar, B.; Purkayastha, P.; Das, P.; Chattopadhyay, N. *Langmuir* **2007**, *23*, 4842.
(18) Mallick, A.; Chattopadhyay, N. *Biophys. Chem.* **2004**, *109*, 261.
(19) Mallick, A.; Haldar, B.; Chattopadhyay, N. *J. Photochem. Photobiol., B* **2005**, *78*, 215.
(20) Mallick, A.; Chattopadhyay, N. *Photochem. Photobiol.* **2005**, *81*, 419.
(21) Varela, A. P.; Burrows, H. D.; Douglas, P.; Miguel, M. G. *J. Photochem. Photobiol., A* **2001**, *146*, 29.
(22) Dias, A.; Varela, A. P.; Miguel, M. G.; Becker, R. S.; Maçanita, A. L.; Burrows, H. D. *J. Phys. Chem.* **1996**, *100*, 17970.
(23) Miguel, M. G.; Burrows, H. D.; Escaroupa, P.; Varela, A. P. *Colloids Surf., A* **2001**, *176*, 85.
(24) Varela, A. P.; Dias, A.; Miguel, M. G.; Becker, R. S.; Maçanita, A. L. *J. Phys. Chem.* **1995**, *99*, 2239.
(25) Chakrabarty, A.; Mallick, A.; Haldar, B.; Das, P.; Chattopadhyay, N. *Biomacromolecules* **2007**, *8*, 920.
(26) Tamoto, Y.; Segawa, H.; Shirota, H. *Langmuir* **2005**, *21*, 3757.
(27) Chakrabarty, D.; Chakrabarty, A.; Seth, D.; Hazra, P.; Sarkar, N. *J. Chem. Phys.* **2005**, *122*, 184516.
(28) Weidemaier, K.; Tavernier, H. L.; Fayer, M. D. *J. Phys. Chem. B* **1997**, *101*, 9352.
(29) Chattopadhyay, N.; Dutta, R.; Chowdhury, M. *J. Photochem. Photobiol., A* **1989**, *47*, 249.
(30) Muller, N. In *Reaction Kinetics in Micelles*; Cordes, E. A., Ed.; Plenum Press: New York, 1973.
(31) Mallick. A.; Haldar, B.; Maiti, S.; Chattopadhyay, N. *J. Colloid. Interface Sci.* **2004**, *278*, 215.
(32) Berr, S.; Jones, R. R. M.; Johnson, J. S. *J. Phys. Chem.* **1992**, *96*, 5611.
(33) Shannigrahi, M.; Bagchi, S. *Chem. Phys. Lett.* **2004**, *396*, 367.

(34) Almgren, M.; Grieser, F.; Thomas, J. K. *J. Am. Chem. Soc.* **1979**, *101*, 279.
(35) Saroja, G.; Ramachandram, B.; Saha, S.; Samanta, A. *J. Phys. Chem. B* **1999**, *103*, 2906.
(36) Macgregor, R. B.; Weber, G. *Nature* **1986**, *319*, 70.
(37) Kossower, E. M.; Kantey, H. *J. Am. Chem. Soc*. **1983**, *105*, 6236.
(38) Sytnik, A.; Kasha, M. *Proc. Natl. Acad. Sci. U.S.A.* **1994**, *91*, 8627.
(39) Reichardt, C. In *Molecular Interactions*; Ratajazak, H., Orville-Thomas, W. J., Eds.; Wiley: New York, 1982; Vol. 3, p 255.
(40) Mallick, A.; Haldar, B.; Maiti, S.; Bera, S. C.; Chattopadhyay, N. *J. Phys. Chem. B* **2005**, *109*, 14675.
(41) Breslow, R.; Guo, T. *Proc. Natl. Acad. Sci. U.S.A.* **1990**, *87*, 167.
(42) Christianziana, P.; Lelj, F.; Amodeo, P.; Barone, G.; Barone, V. *J. Chem. Soc., Faraday Trans. 2* **1989**, *5*, 621.
(43) Makhatadze, G. I.; Privalov, P. L. *J. Mol. Biol.* **1992**, *22*, 6491.
(44) Midura, R. J.; Yanagishita, M. *Anal. Biochem*. **1995**, *228*, 318.
(45) Chattopadhyay, N. *ACH Models Chem*. **1997**, *134*, 129.
(46) Mallick, A.; Haldar, B.; Chattopadhyay, N. *J. Phys. Chem. B* **2005**, *109*, 14683.
(47) Dutt, G. B. *J. Phys. Chem. B* **2004**, *108*, 3651.
(48) Hazra, P.; Chakraborty, D.; Sarkar, N. *Langmuir* **2002**, *18*, 7872.
(49) Das, P.; Mallick, A.; Haldar, B.; Chakrabarty, A.; Chattopadhyay, N. *J. Chem. Phys.* **2006**, *125*, 044516.
(50) Matzinger, S.; Hussey, D. M.; Fayer, M. D. *J. Phys. Chem. B* **1998**, *102*, 7216.
(51) Cang, H.; Brace, D.; Fayer, M. D. *J. Phys. Chem. B* **2001**, *105*, 10007.
(52) Dutt, G. B.; *J. Phys. Chem. B* **2003**, *107*, 10546.